Advances in Materials
2022; 10(4): 85-93
http://www.sciencepublishinggroup.com/j/am
doi: 10.11648/j.am.20221104.12
ISSN: 2327-2503 (Print); ISSN: 2327-252X (Online)

Organic-Inorganic Hybrid Materials: Crystal Growth and XRD Analysis of $[(C_{38}H_{30}N_8)_2{\cdot}CoCl_4]$ and $[(CH_3NH_3)_2{\cdot}CoCl_4]$

Mouhamadou Birame Diop[1, *], Modou Sarr[1], Mouhamadou Sembene Boye[2], Sérigne Cissé[1], Libasse Diop[1], Allen G. Oliver[3], David Renald[4]

[1]Inorganic and Analytical Chemistry Laboratory, Department of Chemistry, Faculty of Science and Technology, Cheikh Anta Diop University, Dakar, Senegal

[2]Department of Physic and Chemistry, Faculty of Science and Technology of Education and Training, Cheikh Anta Diop University, Dakar, Senegal

[3]Department of Chemistry and Biochemistry, University of Notre Dame, Nieuwland, USA

[4]Reactivity and Solid State Chemistry Laboratory, University of Picardie, Jules Verne, Amiens, France

Email address:

mouhamadoubdiop@gmail.com (Mouhamadou Birame Diop)

[*]Corresponding author

To cite this article:

Mouhamadou Birame Diop, Modou Sarr, Mouhamadou Sembene Boye, Sérigne Cissé, Libasse Diop, Allen G. Oliver, David Renald. Organic-Inorganic Hybrid Materials: Crystal Growth and XRD Analysis of $[(C_{38}H_{30}N_8)_2{\cdot}CoCl_4]$ and $[(CH_3NH_3)_2{\cdot}CoCl_4]$. *Advances in Materials*. Vol. 10, No. 4, 2022, pp. 85-93. doi: 10.11648/j.am.20221104.12

Received: October 7, 2022; **Accepted**: October 24, 2022; **Published**: October 30, 2022

Abstract: Two tetrachloridocobaltate (II) hybrid compounds were isolated and structurally characterized by single crystal X-ray crystallography. The compound $[(C_{38}H_{30}N_8)_2{\cdot}CoCl_4]$ (1), crystallizes in the monoclinic space group $P2_1/c$ with $Z = 4$, a = 12.0894(7) Å, b = 15.1839(8) Å, c = 19.8015(11) Å, β = 90.786(2)° and V = 3634.5(3) Å^3. Compound $[(CH_3NH_3)_2{\cdot}CoCl_4]$ (2), crystallizes in the monoclinic space group $P2_1/c$ with $Z = 4$, $a = 7.6385(5)$ Å, $b = 12.6684(8)$ Å, $c = 10.8730(6)$ Å, β = 96.540(2)° and $V = 1045.31(11)$ Å^3. The compound 1 consists of 2,3,5-triphenyltetrazolium cations and tetrachloridocobaltate (II) ions connected through weak C–H···Cl hydrogen bonds affording a 3D structure. Additional π···π interactions consolidate the stability and the compactness of the 3D framework. The tetrazolium (C1N1N2N3N4) ring forms dihedral angles of 85.04(11), 49.37(11) and 27.85(11)° with the planes of the benzene rings of the substituent groups while the tetrazolium (C20N5N6N7N8) ring forms dihedral angles of 52.92(11), 47.37(11) and 9.97(11)° with the planes of the benzene rings of the substituent groups. The compound 2 is composed of methylammonium cations and tetrachloridocobaltate (II) dianions connected by extended N–H···Cl hydrogen bonding patterns giving rise to a 3D structure. The methylammonium cations adopt a general position and are not exceptional. In both structures, the Co centre within the dianion is bonded to four chloride ligands and adopts a distorted tetrahedral geometry. The extensive hydrogen bonding patterns within compound 2 describe $R^2_2(4)$, $R^3_4(410)$, $R^4_4(12)$, $R^5_5(14)$, $R^4_6(14)$, $R^5_6(16)$ and $R^6_6(18)$ rings whereas 1, through the weak C–H···Cl hydrogen bond patterns, generates mainly $R^2_1(4)$ rings and other hydrogen bonds of D type.

Keywords: 2,3,5-Triphenyltetrazolium, Methylammonium; Cobalt (II), Single Crystal X-ray Crystallography, 3D Structure

1. Introduction

The design and synthesis of organic–inorganic hybrid materials, containing the tetrachloridocobaltate (II) dianion with various cobalt (II) complex-cations or organic cations, gained an increasing interest, during the past years, owing to the diversity of structural topologies, and photoelectric behavior, antimicrobial, thermal, absorption, magnetic, optical, electrical and catalysis properties they aroused [1–8]. To date, countless $CoCl_4^{2-}$ hybrid materials with cobalt complex-cation or organic species as counter ion are known [9–17]. However, to our knowledge (CSD), only 16 different crystal structures with 2,3,5-triphenyltetrazolium as counter ion have been reported [18–26]. Indeed, Kawamura and coworkers isolated the hybrid 2,3,5-triphenyltetrazolium dichloro-(1,3,5-triphenylformazanato)-cobalt (ii) [27],

Nakashima and coworkers the hybrid bis (2,3,5-triphenyltetrazolium) tetrakis(isothiocyanato)-cobalt (ii) [28], and Buttrus and coworkers the organic-inorganic hybrid bis (2,3,5-triphenyl-2H-tetrazol-3-ium) tetrachloro-copper (ii) [29], specially. Focusing on this family compounds since a while, the Dakar group has yet reported studies of few organic-inorganic hybrid compounds with tetrachloridocobaltate (II) ion [30, 31], an hybrid complex wherein 2,3,5-triphenyltetrazolium is combined to acetonyltriphenylphosphonium as well [26]. In the course of our ongoing to widen the hybrid family materials, especially those with both tetrachloridocobaltate (II) and 2,3,5-triphenyltetrazolium or mixed counter ions, we investigated, in organic solvents, the reactions between cobalt (II) dichloride hexahydrate, $CoCl_2{\cdot}6H_2O$ and, 2,3,5-triphenyltetrazolium chloride (TTC), $C_{19}H_{15}N_4Cl$ on the one hand, methylammonium chloride, CH_3NH_3Cl and dimethylammonium chloride, $(CH_3)_2NH_2Cl$ on the other hand. These interactions afforded single crystals of compounds $[(C_{19}H_{15}N_4)_2{\cdot}CoCl_4]$ (1) and $[(CH_3NH_3)_2{\cdot}CoCl_4]$ (2) (Figure 1) whose X-ray crystallographic analyses are carried out and reported herein.

2. Experimental

2.1. General

Reagents 2,3,5-triphenyltetrazolium chloride, $C_{19}H_{15}N_4Cl$ ($\geq$ 98% purity), methylammonium chloride, CH_3NH_3Cl (≥99% purity), dimethylammonium chloride, $(CH_3)_2NH_2Cl$ ($\geq$ 98% purity) and cobalt (II) dichloride hexahydrate, $CoCl_2{\cdot}6H_2O$ (98% purity) were purchased from Sigma-Aldrich, Steinheim am Albuch, Germany and were used without any further purification.

2.2. Synthesis of $[(C_{19}H_{15}N_4)_2{\cdot}CoCl_4]$ (1)

The isolation of compound 1 follows a two-step. The one pot reaction in 35 mL of acetonitrile, between two equivalents of 2,3,5-triphenyltetrazolium chloride, $C_{19}H_{15}N_4Cl$ (503mg, 1.50mmol) and one equivalent of cobalt (II) dichloride hexahydrate, $CoCl_2{\cdot}6H_2O$ (179mg, 0.75mmol) yielded a blue clear solution which was subsequently submitted to slow solvent evaporation at room temperature (305K), affording a blue powder after some days.

Recrystallization of an amount of the blue powder (200mg, 0.25mmol) in 25 mL acetone solvent afforded green block-like crystals suitable for a single-crystal X-ray diffraction study, after some days of slow solvent evaporation at room temperature (305 K) and finally characterized as 1.

2.3. Synthesis of $[(CH_3NH_3)_2{\cdot}CoCl_4]$ (2)

Compound 2 was isolated by mixing, in a 2:1:1 molar ratio, methylammonium chloride CH_3NH_3Cl (123mg, 1.82mmol), dimethylammonium chloride $(CH_3)_2NH_2Cl$ (74mg, 0.91mmol) and cobalt (II) dichloride hexahydrate, $CoCl_2{\cdot}6H_2O$ (217mg, 0.91mmol) in 50 mL of acetonitrile. A clear blue solution was obtained, and allowed to evaporate at room temperature (305K). After some days, blue platelet-like crystals suitable for a single-crystal X-ray diffraction study, were obtained from the supernatant solution and characterized as 2. The aim was to isolate an organic-inorganic hybrid compound with mixed counter ions composed of methylammonium and dimethylammonium.

The proposed equations of the reactions leading to the isolation of compounds 1 and 2 are shown in Figure 1.

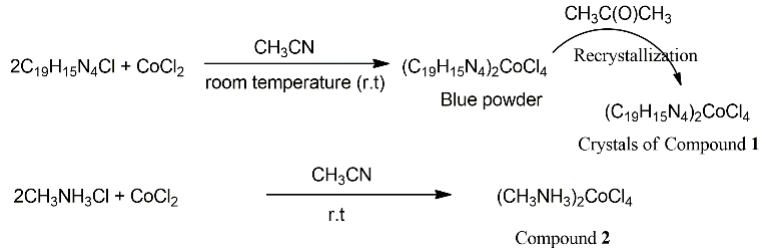

Figure 1. *Proposed equation of reactions of the synthesis of compound 1.*

2.4. X-ray Crystallography

For 1, crystal of approximate dimensions 0.190×0.184×0.100 mm was used for data collection. The X-ray crystallographic data for 1 were collected using a Bruker Kappa X8-APEX-II diffractometer at T = 120 (2) K. Data were measured using φ and ω scans using MoKα radiation (λ = 0.71073 Å) using a collection strategy to obtain a hemisphere of unique data determined by Apex2 [32]. Data were corrected for absorption and polarization effects using intensity measurements by SADABS [33]. Cell parameters were determined and refined using the SAINT program [34]. The structure was solved by intrinsic phasing methods using SHELXT-2014/2 [35] and the structure refined using least-squares minimization SHELXL-2014/7 [36].

For 2, a crystal of approximate dimensions 0.10×0.05×0.02 mm was used for data collection. The X-ray crystallographic data for compound 2 were collected using a Bruker D8 Venture diffractometer at T = 296 (2) K. Data were measured using φ scans using MoKα radiation (λ = 0.71073 Å) using a collection strategy to obtain a hemisphere of unique data determined by Bruker D8 Venture. Data were analytically corrected for absorption and polarization effects [37]. Cell parameters were determined and refined using the SAINT program [34]. The structure was solved by the direct method using SHELXS

[38] and the structure refined using least-squares minimization SHELXL-2018/3 [36].

Programs used for the representation of the molecular and crystal structures: Olex2 [39] and Mercury [40]. Crystal data, data collection and structure refinement details for 1 are summarized in Table 1. Selected bond lengths and angles are listed in Tables 2 and 3, respectively.

CCDC 2211660 (1) and 2211661 (2) contain the supplementary crystallographic data for this paper. Copies of these data can be obtained free of charge from the Cambridge Crystallographic Data Centre (CCDC), 12 Union Road, Cambridge CB2 1EZ, UK.

Table 1. *Crystal data and structure refinement of compounds 1 and 2.*

Parameters	Compound	
	1	**2**
Empirical Formula	$C_{38}H_{30}Cl_4CoN_8$	$C_2H_{12}Cl_4CoN_2$
Formula weight	799.43	264.87
Temperature (K)	120 (2)	296 (2)
Crystal system	Monoclinic	Monoclinic
Space group	$P2_1/c$	$P2_1/c$
a, (Å)	12.0894(7)	7.6385(5)
α, (°)	90	90
b, (Å)	15.1839(8)	12.6684(8)
β, (°)	90.786(2)	96.540 (2)
c, (Å)	19.8015(11)	10.8730(6)
γ, (°)	90	90
Volume (Å^3)	3634.5(3)	1045.31(11)
Z	4	4
ρ_{calc} (g/cm^3)	1.461	1.683
μ (mm^{-1})	0.807	2.599
F(000)	1636	532
Crystal size (mm^3)	0.190 × 0.184 × 0.100	0.10 × 0.05 × 0.02
Radiation (Å)	MoKα (λ = 0.71073)	MoKα (λ = 0.71073)
2Θ range for data collection (°)	3.159–36.343	2.478–33.122
Index ranges	$-14 \le h \le 16$ $-20 \le k \le 19$ $-26 \le l \le 26$	$-11 \le h \le 11$ $-19 \le k \le 19$ $-16 \le l \le 16$
Reflections collected	63695	102055
Independent reflections	9108 [Rint = 0.0387]	3828 [Rint = 0.0369]
Data/restraints/parameters	9108/0/460	3828/0/130
Goodness-of-fit on F^2	1.057	1.086
Final R indexes [$I > 2\sigma(I)$]	R1 = 0.0416 wR2 = 0.1078	R1 = 0.0357 wR2 = 0.0683
Final R indexes [all data]	R1 = 0.0525 wR2 = 0.1139	R1 = 0.0541 wR2 = 0.0753
Largest diff. peak/hole (e Å^{-3})	2.200 and -0.291	0.980 and -0.691

R1 = $\Sigma(||F_o|-|F_c||)/\Sigma|F_o|$; wR2 = $[\Sigma w(F_o^2-F_c^2)^2/\Sigma[w(F_o^2)^2]^{1/2}$ where $w = 1/[\sigma^2(F_o^2) + 2.5412P+(0.0596P)^2]$ for **1** and $w = 1/[\sigma^2(F_o^2) + 0.8278P+(0.0256P)^2]$ for **2** where $P = (F_o^2)+2F_c^2)/3$; [c] goodness of fit = $[\Sigma w(F_o^2-F_c^2)^2/(N_o-N_v)]^{1/2}$.

3. Results and Discussion

3.1. Crystal and Molecular Structure of [$(C_{19}H_{15}N_4)_2$·$CoCl_4$] (1)

The organic-inorganic hybrid complex 1, [$(C_{19}H_{15}N_4)_2$·$CoCl_4$], crystallizes as green block-like crystals in the monoclinic space group $P2_1/c$. The asymmetric unit depicted in Figure 2, consists of one tetrachloridocobaltate (II) dianion and two 2,3,5-triphenyltetrazolium ions. The terachloridocobaltate (II) dianion's geometric parameters within compound 1 varying from 2.2604(6) to 2.2918(6) Å and from 106.03(2) to 115.35(2)° well corroborate, as earlier encountered [9–17], a distorted tetrahedron about Co centre. In 2018, the Dakar group has reported a copper (II) complex with mixed counter ions comprising 2,3,5-triphenyltetrazolium cation exhibiting a π delocalization for the tetrazolium ring [26].

The N–N and C–N bond distances of the two 2,3,5-triphenyltetrazolium ions from 2.296 (2) to 1.340(3) Å and from 2.306(2) to 2.334(3) Å, compare well and are in accordance with the published values evidencing a π delocalization within the tetrazolium rings [18–26].

The inter-species weak C–H···Cl hydrogen bonds (see table 4 for details) present in compound 1 afford $R_1^2(4)$ rings and multiple other hydrogen bonds of D type (see Figure 3).

In the crystal structure, in addition to the weak C–H···Cl hydrogen bond patterns, the 2,3,5-triphenyltetrazolium cation (C1N1N2N3N4) exhibits π···π interactions with the centroid to centroid distance being 3.6590 (13) Å between the phenyl ring C14 to C19 and its closest symmetry equivalent, and 3.5595 (13) Å between the phenyl ring C8 to C13 and its closest symmetry equivalent, affording a three-dimensional network (Figure 4).

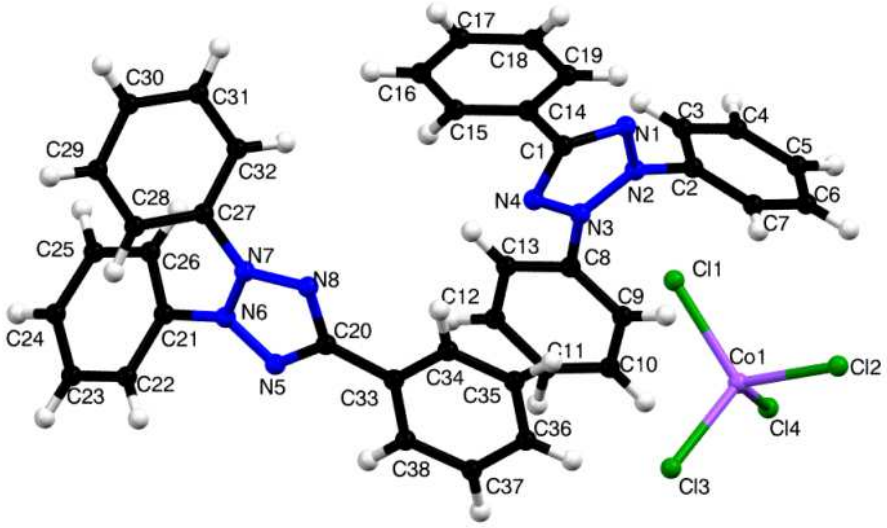

Figure 2. *Molecular view of 1 showing 50% probability ellipsoids for atoms and the crystallographic numbering scheme adopted [atom color code: C, black; H, white; N, blue; Cl, green; Co, mauve].*

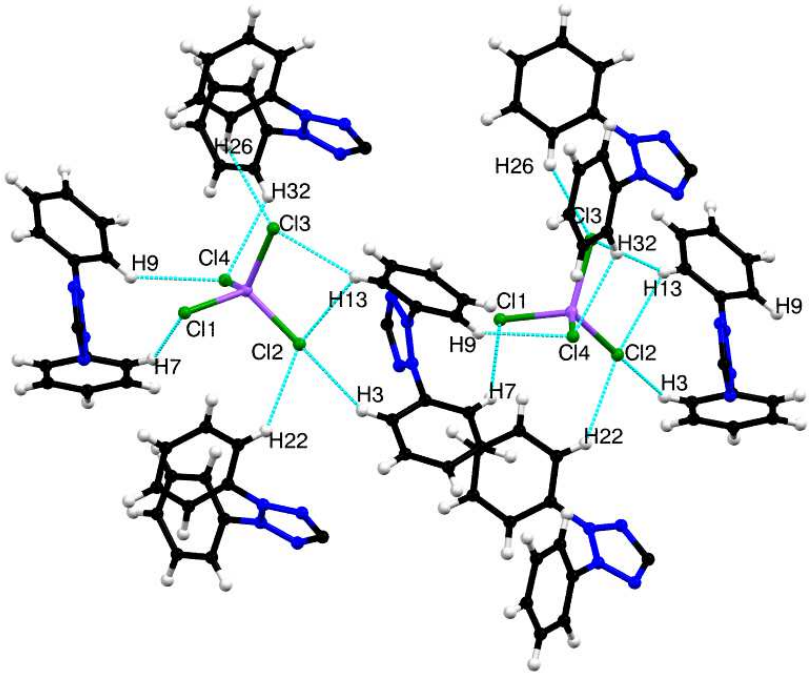

Figure 3. *Molecular view of 1 showing 50% probability ellipsoids for atoms, showing the interconnections between the species. The phenyl ring which is not involved in C–H···Cl hydrogen bonds is omitted for clarity. Hydrogen bonds are represented as turquoise dashed lines [atom color code: C, black; H, white; N, blue; Cl, green; Co, mauve].*

3.2. Crystal and Molecular Structure of [$(CH_3NH_3)_2{\cdot}CoCl_4$] (2)

Daub and coworkers reported, in 2016, the synthesis, crystal structure, and optical properties the hybrid $[(CH_3NH_3)_2{\cdot}CoCl_4]$, with final R indexes *R1* = 0.046, *wR2* = 0.087 and *R1* (all data) = 0.074 [2]. In 2019, Yin and coworkers reported the crystal structure, absorption properties, photoelectric behavior of the organic–inorganic hybrid $[(CH_3NH_3)_2{\cdot}CoCl_4]$, with final R indexes *R1* = 0.0446, *wR2* = 0.1316, *R1* (all data) = 0.0526 and *wR2* (all data) = 0.1350 [3]. The final R indexes for this organic–inorganic hybrid $[(CH_3NH_3)_2{\cdot}CoCl_4]$ (2) are *R1* = 0.0357, *wR2* = 0.0683, *R1* (all data) = 0.0541 and *wR2* (all data) = 0.0753. This study is focused on the supramolecular point of view of the organic-inorganic hybrid $[(CH_3NH_3)_2{\cdot}CoCl_4]$. The compound 2, $[(CH_3NH_3)_2{\cdot}CoCl_4]$, crystallizes as blue platelet-like crystals in the monoclinic space group $P2_1/c$. The asymmetric unit, depicted in Figure 5, is comprised of a tetrachloridocobaltate (II) anion and two methylammonium counter ions, chemically identical, yet different. The difference between N1 and N2 cations consists in their involvement in hydrogen bonding patterns.

The C–N length values (see Table 2) are in agreement with

the published values for alkylammonium containing compounds [2, 3, 41]. The geometric parameters within the terachloridocobaltate (II) dianions, varying from 2.2645(6) to 2.2753(6) Å and from 105.80(2) to 112.52(2)° are comparable to those in 1, thus evidencing a distorted tetrahedron [9–17].

The inter-species hydrogen bonding patterns (Table 5) exhibit each dianion to be in interaction with seven cations (see Figure 6): four N1 counter ions and three N2 ones. Within these H-bond interactions, chlorine atoms, except Cl2 connected to only N1 cation, are linked to two counter ions, homogeneously for Cl1 (two N1 cations) and Cl3 (two N2 cations) however heterogeneously for Cl4 (one N1 and one N2 cations) (Figure 6). Thus, N1 counter ion is hydrogen bonded to four tetrachloridocobaltate (II) ions through two dissymmetrical N1–H1*C*···Cl1, one N1–H···Cl2 and one N1–H···Cl4 (see Figure 7 and table 5). Contrary to N1 counter ion, the latter N2 cation is hydrogen bonded to three tetrachloridocobaltate (II) ions *via* two different N2–H···Cl3 and one N2–H···Cl4 (see Figure 8 and table 5). In compound 2, the extensive inter-species hydrogen bonding interactions between dianions and counter ions exhibit six hydrogen bonded ring patterns: $R_2^2(4)$, $R_4^3(10)$, $R_4^4(12)$, $R_5^5(14)$, $R_6^4(14)$, $R_6^5(16)$ and $R_6^6(18)$. The two dissymmetrical N1–H2*C*···Cl2 hydrogen bonds are both involved in the $R_2^2(4)$ ring formed by two tetrachloridocobaltate (II) and two N1 methylammonium ions (Figure 9). Similarly to the $R_2^2(4)$ ring, the hydrogen bonded macrocycles $R_4^3(10)$ and $R_4^4(12)$ are built from interactions between four species: two tetrachloridocobaltate (II) and, one N1 and N2 methylammonium species for $R_4^3(10)$ (Figure 10a), two N2 methylammonium cations $R_4^4(12)$ (Figure 10b). In the contrary, the other H-bonded macrocycles are comprised of six species among with three tetrachloridocobaltate (II) ions and, one N1 and two N2 methylammonium ions for $R_5^5(14)$ and $R_6^4(14)$ (Figure 10c and d), two N1 and one N2 counter ions for $R_6^5(16)$ and $R_6^6(18)$ (Figure 11a and b).

The extended hydrogen bonding interconnections between tetrachloridocobaltate (II) dianions and methylammonium counter ions afforded a supramolecular 3D framework depicted in Figure 12.

Table 2. *Selected prominent distances (Å) for compounds 1 and 2.*

Compound 1			
Atom-Atom	Bond length	Atom-Atom	Bond length
Co1–Cl4	2.2604 (6)	N4–C1	1.340 (3)
Co1–Cl1	2.2749 (6)	C1–C14	1.452 (3)
Co1–Cl2	2.2829 (6)	N5–N6	1.306 (2)
Co1–Cl3	2.2918 (6)	N5–C20	1.334 (3)
N1–N2	1.307 (2)	N6–N7	1.330 (2)
N1–C1	1.339 (3)	N6–C21	1.440 (2)
N2–N3	1.330 (2)	N7–N8	1.306 (2)
N2–C2	1.440 (3)	N7–C27	1.437 (2)
N3–N4	1.296 (2)	N8–C20	1.340 (3)
N3–C8	1.439 (3)	C20–C33	1.450 (3)
Compound 2			
Atom-Atom	Bond length	Atom-Atom	Bond length
Co1–Cl4	2.2735 (5)	Co1–Cl1	2.2646 (6)
Co1–Cl3	2.2754 (6)	N1–C1	1.440 (4)
Co1–Cl2	2.2686 (5)	N2–C2	1.451 (3)

Table 3. *Selected prominent angle values (°) for compounds 1 and 2 [Symmetry codes: (ii) x +1/2, y, −z+1/2].*

Compound 1			
Atom-Atom-Atom	Angle value	Atom-Atom-Atom	**Angle value**
Cl4–Co1–Cl1	106.03 (2)	N4–N3–N2	110.28 (16)
Cl4–Co1–Cl2	109.57 (2)	N3–N4–C1	103.87 (16)
Cl1–Co1–Cl2	110.02 (2)	N1–C1–N4	112.35 (17)
Cl4–Co1–Cl3	115.35 (2)	N6–N5–C20	103.98 (16)
Cl1–Co1–Cl3	107.73 (2)	N5–N6–N7	109.72 (16)
Cl2–Co1–Cl3	108.07 (2)	N8–N7–N6	110.29 (15)
N2–N1–C1	103.54 (16)	N7–N8–C20	103.48 (16)
N1–N2–N3	109.96 (16)	N5–C20–N8	112.51 (17)
Compound 2			
Atom-Atom-Atom	Angle value	Atom-Atom-Atom	Angle value
Cl4–Co1–Cl3	112.51 (2)	Cl1–Co1–Cl4	108.65 (2)
Cl2–Co1–Cl4	110.03 (2)	Cl1–Co1–Cl3	109.51 (3)
Cl2–Co1–Cl3	105.80 (2)	Cl1–Co1–Cl2	110.32 (2)

Table 4. *Hydrogen-bonds geometry in the crystal of 1 [Symmetry codes: (i) x, −y+1/2, z−1/2; (ii) x−1, −y+1/2, z−1/2].*

D–H···A	***d* (*D*-H)**	***d* (H···*A*)**	***d* (*D*···*A*)**	**∠(*D*-H···*A*)**
C3–H3···Cl2^{i}	0.95	2.88	3.723 (3)	148.2
C7–H7···Cl1	0.95	2.92	3.696 (2)	140.2
C9–H9···Cl4	0.95	2.89	3.682 (2)	142.1
C13–H13···Cl2^{i}	0.95	2.93	3.561 (2)	125.2
C13–H13···Cl3^{i}	0.95	2.89	3.755 (2)	151.6
C22–H22···Cl2^{ii}	0.95	2.87	3.593 (2)	133.9
C26–H26···Cl3^{i}	0.95	2.91	3.644 (2)	135.4
C32–H32···Cl4^{i}	0.95	2.88	3.486 (2)	122.6

Table 5. *Hydrogen-bonds geometry in the crystal of **2** [Symmetry codes: (i) x, −y+1/2, z+1/2; (ii) –x+2, –y, −z+1; (iii) −x+1, −y, −z+1; (iv) −x+1, y+1/2, −z+1/2].*

D–H···A	***d* (*D*-H)**	***d* (H···*A*)**	***d* (*D*···*A*)**	**∠(*D*-H···*A*)**
N1–H1A···Cl4^{i}	0.83(5)	2.80(5)	3.524(4)	146(4)
N1–H1B···Cl2^{ii}	0.80(5)	2.65(5)	3.345(4)	147(5)
N1–H1C···Cl1	0.93(6)	2.71(7)	3.323(3)	124(5)
N1–H1C···Cl1^{iii}	0.93(6)	2.66(7)	3.415(4)	139(5)
N2–H2A···Cl4^{i}	0.84(4)	2.41(4)	3.243(2)	174(3)
N2–H2B···Cl3^{iv}	0.88(3)	2.49(3)	3.273(2)	149(3)
N2–H2C···Cl3^{iii}	0.86(4)	2.53(3)	3.289(2)	147(3)

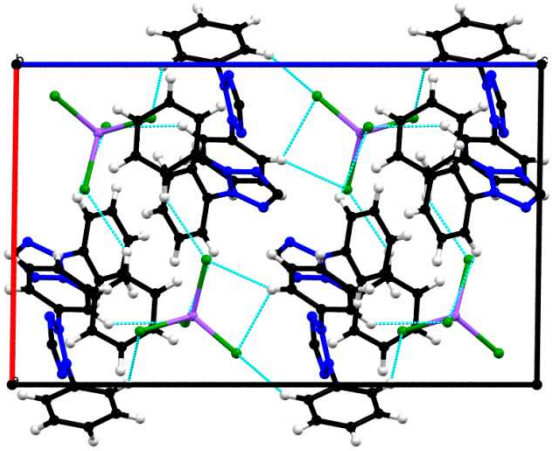

Figure 4. *Molecular packing diagram of 1 showing 50% probability ellipsoids for atoms, along the crystallographic b axis showing the three-dimensional network. The phenyl ring which is not involved in C–H···Cl hydrogen bonds is omitted for clarity. Hydrogen bonds are represented as turquoise dashed lines [atom color code: C, black; H, white; N, blue; Cl, green; Co, mauve].*

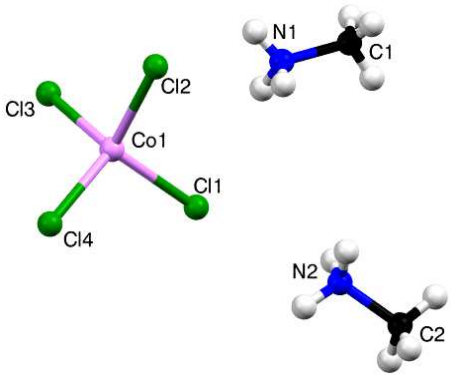

Figure 5. *Molecular view of 2 showing 50% probability ellipsoids for atoms and the crystallographic numbering scheme adopted [atom color code: C, black; H, white; N, blue; Cl, green; Co, mauve].*

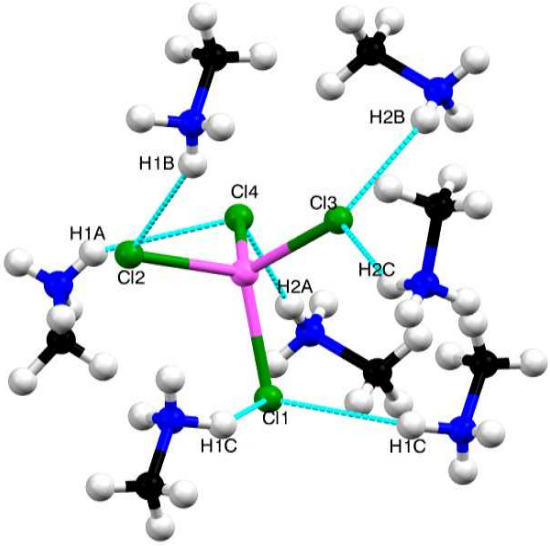

Figure 6. *Molecular view of 2 showing 50% probability ellipsoids for atoms, showing the surrounding of the dianion. Hydrogen bonds are represented as turquoise dashed lines [atom color code: C, black; H, white; N, blue; Cl, green; Co, mauve].*

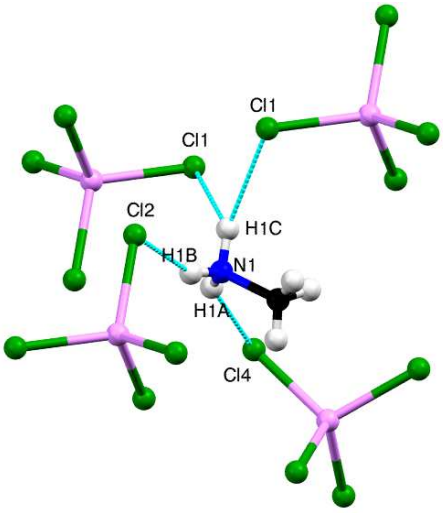

Figure 7. *Molecular view of 2 showing 50% probability ellipsoids for atoms, showing the surrounding of N1 counter ion. Hydrogen bonds are represented as turquoise dashed lines [atom color code: C, black; H, white; N, blue; Cl, green; Co, mauve].*

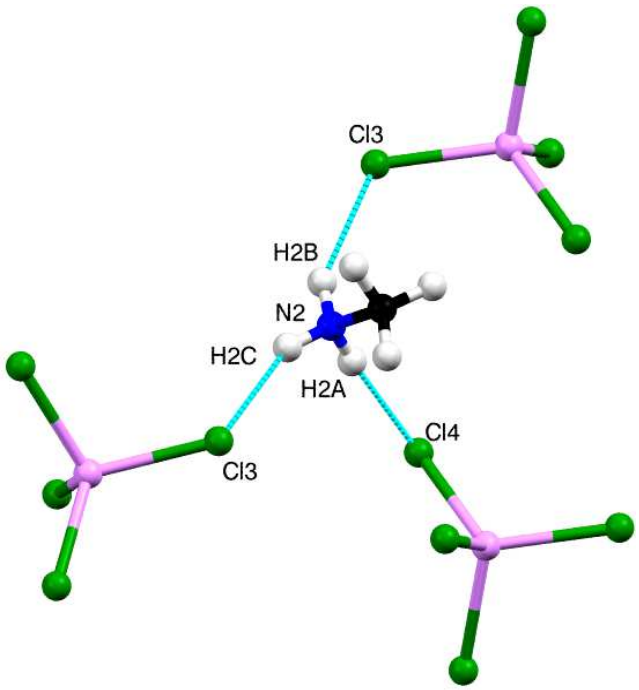

Figure 8. *Molecular view of 2 showing 50% probability ellipsoids for atoms, showing the surrounding of N2 counter ion. Hydrogen bonds are represented as turquoise dashed lines [atom color code: C, black; H, white; N, blue; Cl, green; Co, mauve].*

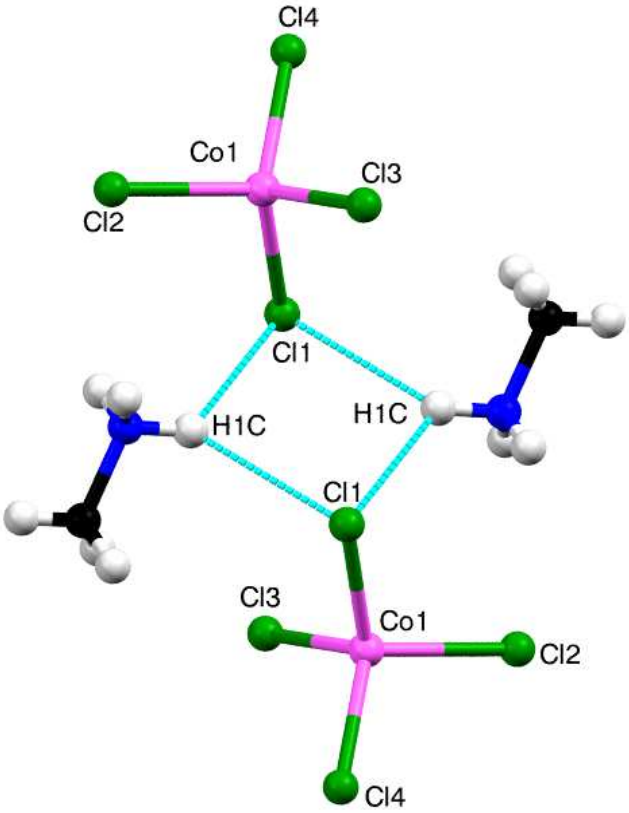

Figure 9. *View of 2 showing 50% probability ellipsoids for atoms, showing the $R_2^2(4)$ ring. Hydrogen bonds are represented as turquoise dashed lines [atom color code: C, black; H, white; N, blue; Cl, green; Co, mauve].*

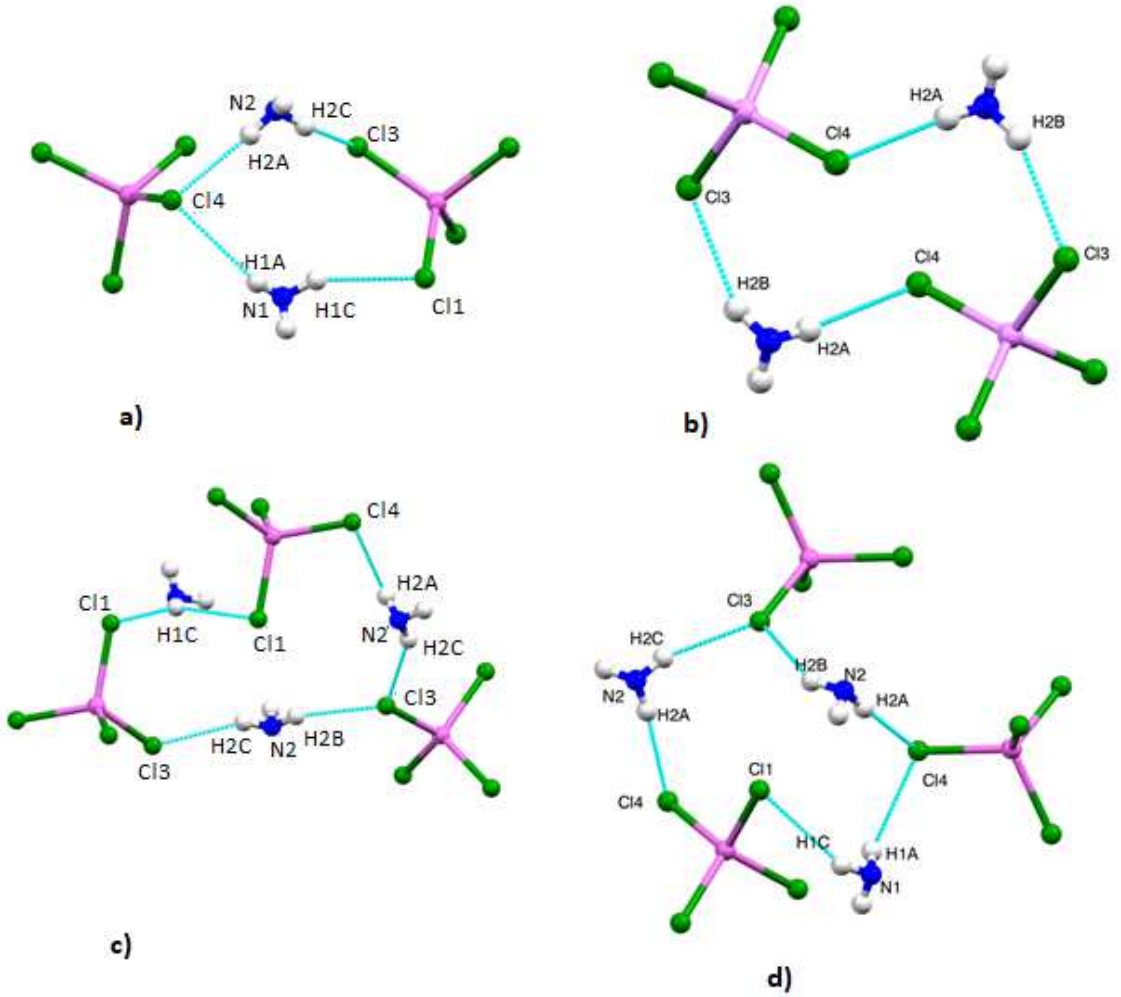

Figure 10. *View of 2 showing 50% probability ellipsoids for atoms, showing* $R_4^3(10), R_4^4(12)$, $R_5^5(14)$ *and* $R_6^4(14)$ *rings. Hydrogen bonds are represented as turquoise dashed lines [atom color code: C, black; H, white; N, blue; Cl, green; Co, mauve]. Methyl groups are omitted for clarity.*

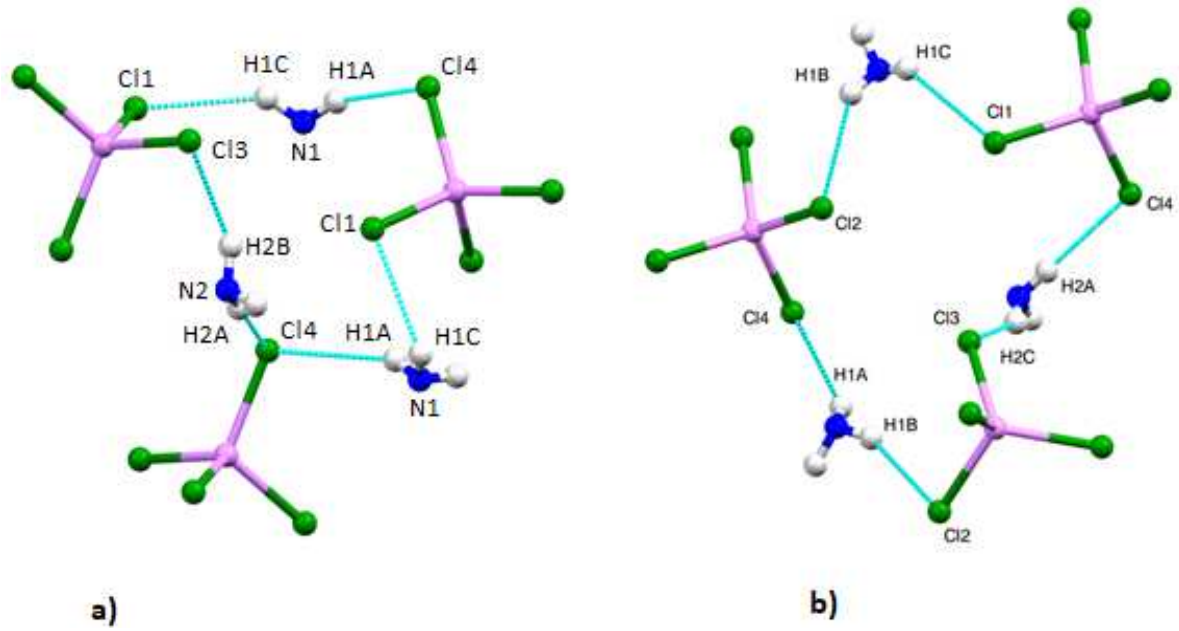

Figure 11. *View of 2 showing 50% probability ellipsoids for atoms, showing* $R_6^5(16)$ *and* $R_6^6(18)$ *rings. Hydrogen bonds are represented as turquoise dashed lines [atom color code: C, black; H, white; N, blue; Cl, green; Co, mauve]. Methyl groups are omitted for clarity.*

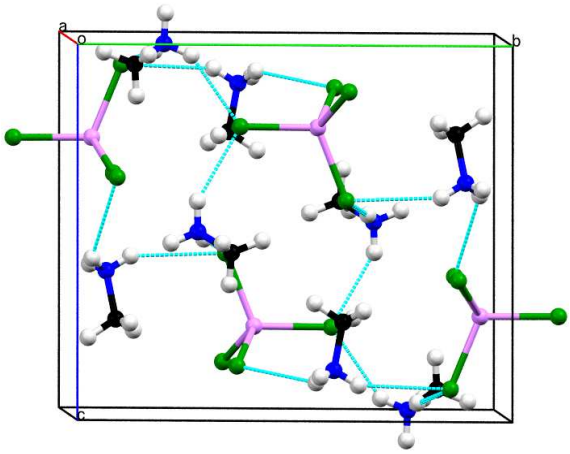

Figure 12. *Molecular packing diagram of 2 showing 50% probability ellipsoids for atoms, showing the 3D framework.*

4. Conclusion

Two 2,3,5-triphenyltetrazolium and methylammonium salts of tetrachloridocobaltate (II) have been synthesized by one pot reaction and structurally investigated by single crystal X-ray diffraction analysis. The tetrachloridocobaltate (II) ion's geometry is a distorted tetrahedron for the two studied compounds. Compound 1 exhibits only $R_1^2(4)$ rings, hydrogen bonds of D type and $\pi\cdots\pi$ interactions. Compound 2 as regards describes extended hydrogen bonding interactions which yield seven ring types *ie* $R_2^2(4)$, $R_4^3(10)$, $R_4^4(12)$, $R_5^5(14)$, $R_6^4(14)$, $R_6^5(16)$ and $R_6^6(18)$. In both compounds 1 and 2, the weak hydrogen bond interconnections give rise to a 3D structure. Further attempts, to isolate and characterize new organic-inorganic hybrids of both methylammonium and 2,3,5-triphenyltetrazolium with several metal reagents, are in progress.

Acknowledgements

The authors acknowledge the Cheikh Anta Diop University of Dakar (Senegal), the University of Notre Dame (USA) and the University of Picardie (France) for equipment facilities.

References

[1] Amamou, W., Essalhi, R., Chniba-Boudjada, N., Zouari, F. (2022). Synthesis, crystal structure, Hirshfeld surface analysis and magnetic studies of bis [1,3-dicyclohexyl-2-ethyl isouronium] tetrachlorocobaltate (II), Journal of Molecular Structure, 1252, 132089. doi: 10.1016/j.molstruc.2021.132089.

[2] Daub, M., Stroh, R., Hillebrecht, H. (2016). Synthesis, Crystal Structure, and Optical Properties of $(CH_3NH_3)_2CoX_4$ (X = Cl, Br, I, $Cl_{0.5}Br_{0.5}$, $Cl_{0.5}I_{0.5}$, $Br_{0.5}I_{0.5}$). Zeitschrift Fur Anorganische Und Allgemeine Chemie, 642, 268-272. 10.1002/zaac.201500738.

[3] Yin, J., Liu, X., Fan, L., Wei, J., He, G., Shi, S., Guo, J., Yuan, C., Chai, N., Wang, C., Cui, J., Wang, X., Zhou, H., Tian, D. (2019). Synthesis, crystal structure, absorption properties, photoelectric behavior of organic–inorganic hybrid $(CH_3NH_3)_2CoCl_4$. Applied Organometallic Chemistry, 33 (4), e4795. doi: 10.1002/aoc.4795.

[4] Mărutescu, L., Calu, L., Chifiriuc, M. C., Bleotu, C., Daniliuc, C.-G., Fălcescu, D., Kamerzan, C. M., Badea, M., Olar, R. (2017). Synthesis, Physico-chemical Characterization, Crystal Structure and Influence on Microbial and Tumor Cells of Some Co (II) Complexes with 5,7-Dimethyl-1,2,4-triazolo [1,5-a] pyrimidine. Molecules, 22, 1233. doi: 10.3390/molecules22071233.

[5] Maha, M., Janzen, D. E., Mohamed, R., Wajda, S. (2016). Synthesis, Crystal Structure, Thermal Analysis, Spectroscopic, and Magnetic properties of a Novel Organic Cation Tetrachlorocobaltate (II). Journal of Superconductivity and Novel Magnetism, 29 (6), 1573-1581. doi: 10.1007/s10948-016-3451-0.

[6] Tounsi, A., Hamdi, B., Zouari, R., Salah, A. B. (2016). DFT (B3LYP/LanL2DZ), non-linear optical and electrical studies of a new hybrid compound: $[C_6H_{10}(NH_3)_2]CoCl_4{\cdot}H_2O$. Physica E, 84, 384-394. doi: 10.1016/j.physe.2016.07.025.

[7] Gong, D., Jia, W., Chen, T., Huang, K.-W. (2013). Polymerization of 1,3-butadiene catalyzed by pincer cobalt (II) complexes derived from 2-(1-arylimino)-6-(pyrazol-1-yl)pyridine ligands. Applied Catalysis A, 464, 35-42. doi: 10.1016/j.apcata.2013.04.026.

[8] Ai, P., Chen, L., Jie, S., Li, B.-G. (2013). Polymerization of 1,3-butadiene catalyzed by ion-pair cobalt complexes with (benzimidazolyl)pyridine alcohol ligands. Journal of Molecular Catalysis A: Chemical, 380, 1-9. doi: 10.1016/j.molcata.2013.09.007.

[9] Liu, M., McGillicuddy, R. D., Vuong, H., Tao, S., Slavney, A. H., Gonzalez, M. I., Billinge, S. J. L., Mason, J. A. (2021). Network-Forming Liquids from Metal–Bis (acetamide) Frameworks with Low Melting Temperatures. Journal of the American Chemical Society, 143 (7), 2801-2811. doi: 10.1021/jacs.0c11718.

[10] Abozeid, S. M., Asik, D., Sokolow, G. E., Lovell, J. F., Nazarenko, A. Y., Morrow, J. R. (2020). Co^{II} Complexes as Liposomal CEST Agents. Angewandte Chemie International Edition, 59 (29), 12093-12097. doi: 10.1002/anie.202003479.

[11] Miecznikowski, J. R., Jasinski, J. P., Kaur, M., Bonitatibus, S. C., Almanza, E. M., Kharbouch, R. M., Zygmont, S. E., Landy, K. R. (2020). Preparation of SNS Cobalt (II) Pincer Model Complexes of Liver Alcohol Dehydrogenase. Journal of Visualized Experiments, 157, e60668. doi: 10.3791/60668.

[12] Vassilyeva, O. Y., Buvaylo, E. A., Kokozay, V. N., Skelton, B. W., Rajnak, C., Titis, J., Boca, R. (2019). Long magnetic relaxation time of tetracoordinate Co^{2+} in imidazo [1,5-a] pyridinium-based $(C_{13}H_{12}N_3)_2[CoCl_4]$ hybrid salt and $[Co(C_{13}H_{12}N_3)Cl_3]$ molecular complex. Dalton Transactions, 48 (30), 11278-11284. doi: 10.1039/C9DT01642B.

[13] Moussa, O. B., Chebbi, H., Zid, M. F. (2019). Synthesis, crystal structure, vibrational study, optical properties and Hirshfeld surface analysis of bis (2,6-diaminopyridinium) tetrachloridocobaltate (II) monohydrate. Journal of Molecular Structure, 1180, 72-80. doi: 10.1016/j.molstruc.2018.11.077.

[14] Said, M., Boughzala, H. (2020). Synthesis, crystal structure, vibrational study, optical properties and thermal behavior of a new hybrid material bis (3-amino-4-phenyl-1H-pyrazolium) tetrachloridocobaltate (II) monohydrate. Journal of Molecular Structure, 1203, 127413. doi: 10.1016/j.molstruc.2019.127413.

[15] Zhilyaeva, E. I., Shilov, G. V., Torunova, S. A., Akimov, A. V., Tokarev, S. V., Konarev, D. V., Flakina, A. M., Lyubovskii, R. B., Aldoshin, S. M., Lyubovskaya, R. N. (2020). Structure and properties of ET charge transfer salts with cobalt (II)/zinc (II) anion networks templated by urea. Inorganica Chimica Acta, 505, 119483. doi: 10.1016/j.ica.2020.119483.

[16] Abdelkader, M. M., Abdelmohsen, M., Aboud, A. I. (2021). Crystal structure, magnetic susceptibility, dielectric permittivity, and phase transition in a new organic–inorganic hybrid perovskite (n- C_8 $H_{17}NH_3)_2CoCl_4$. Chem. Phys. Lett., 770, 138423. doi: 10.1016/j.cplett.2021.138423.

[17] Landolsi, M., Abid, S. (2021). Crystal structure and Hirshfeld surface analysis of trans-2,5-dimethylpiperazine-1,4-diium tetrachloridocobaltate (II). Acta Crystallographica, E77 (4), 424-427. doi: 10.1107/S2056989021002954.

[18] Gjikaj, M., Xie, T., Brockner, W. (2009). Uncommon Compounds in Antimony Pentachloride – Ionic Liquid Systems: Synthesis, Crystal Structure and Vibrational Spectra of the Complexes [TPT] [$SbCl_6$] and [Cl-EMIm] [$SbCl_6$]. Zeitschrift für Anorganische und Allgemeine Chemie, 635 (6-7), 1036–1040. doi: 10.1002/zaac.200801392.

[19] Xie, T., Brockner, W., Gjikaj, M. (2009). Formation and Crystal Structure of 2,3,5-Triphenyltetrazolium Hexachlorophosphate and Dichlorophosphate (V), $[TPT]^+[PCl_6]^-$ and $[TPT]^+[PO_2Cl_2]^-$. Zeitschrift für Naturforschung, b64, 989–994. doi: 10.1515/znb-2009-0901.

[20] Golovanov, D. G., Perekalin, D. S., Yakovenko, A. A., Antipin, M. Y., Lyssenko, K. A. (2005). The remarkable stability of the $Cl^{-}\cdots(\pi$-system) contacts in 2,3,5-triphenyltetrazolium chloride. Mendeleev Communications, 15 (6), 237–239. doi: 10.1070/MC2005v015n06ABEH002184.

[21] Fun, H.-K., Chia, T. S., Mostafa, G. A. E., Hefnawy, M. M., Abdel-Aziz, H. A. (2012). 2,3,5-Triphenyl-2H-tetra-zol-3-ium bromide ethanol monosolvate. Acta Crystallographica, E68, o2566. doi: 10.1107/S1600536812032953.

[22] Fun, H.-K., Chia, T. S., Mostafa, G. A. E., Hefnawy, M. M., Abdel-Aziz, H. A. (2012). 2,3,5-Triphenyl-2H-tetra-zol-3-ium tetra-phenyl-borate. Acta Crystallographica, E68, o2567. doi: 10.1107/S1600536812032941.

[23] Ghabbour, H. A., AlRuqi, O. S., Mostafa, G. A. E. (2017). The crystal structure of 2,3,5-triphenyl-2,3-dihydro-1H-tetrazol-1-ium 2,3-dioxoindoline-5-sulfonate, $C_{27}H_{19}N_5O_5S$. Zeitschrift für Kristallographie, 232 (4), 603–605. doi: 10.1515/ncrs-2016-0366.

[24] Fun, H.-K., Chia, T. S., Mostafa, G. A. E., Abunassif, M. M., Abdel-Aziz, H. A. (2012). 2,3,5-Triphenyl-2H-tetra-zol-3-ium iodide. Acta Crystallographica, E68, o2621. doi: 10.1107/S1600536812033661.

[25] Gjikaj, M., Xie, T., Brockner, W. (2009). Synthesis, Crystal Structure and Vibrational Spectrum of 2,3,5-Triphenyltetrazolium Hexachloridoniobate (V) and Oxidotetrachloridoniobate (V) Acetonitrile, [TPT][$NbCl_6$] and [TPT][$NbOCl_4(CH_3CN)$]. Zeitschrift für Anorganische und Allgemeine Chemie, 635 (13-14), 2273–2278. doi: 10.1002/zaac.200900174.

[26] Diop, M. B., Diop, L., Oliver, A. G. (2018). Acetonyltriphenylphosphonium 2,3,5-triphenyltetrazolium tetrachloridocuprate (II). Acta Crystallographica, E74, 69–71. doi: 10.1107/S205698901701800X.

[27] Kawamura, Y., Yamauchi, J., Azuma, N. (1997). Molecular and Crystal Structure of the Complex Composed of 2,3,5-Triphenyltetrazolium Cation and Dichloro-(1,3,5-triphenylformazanato) cobaltate (II) Anion. Acta Crystallographica, B53, 451–456. doi: 10.1107/S0108768196015960.

[28] Nakashima, K., Kawame, N., Kawamura, Y., Tamada, O., Yamauchi, J. (2009). Bis(2,3,5-triphenyl-tetra-zolium) tetra-thio-cyanato-cobaltate (II). Acta Crystallographica, E65, m1406–m1407. doi: 10.1107/S1600536809041464.

[29] Buttrus, N. H., Alyass, J. M., Mohammad, A. F. (2013). Synthesis, Characterization of Mn^{2+}, Co^{2+}, Ni^{2+}, Cu^{2+} and Zn^{2+} Complex Salts with 2,3,5-(Triphenyl) Tetrazolium Chloride and the Crystal Structure of $[CN_4(C_6H_5)_3]_2[CuCl_4]$. Journal of Chemistry and Chemical Engineering, 7, 613–620. doi: 10.17265/1934-7375/2013.07.004.

[30] Diop, M. B., Diop, L., Maris, T. (2015). Crystal structure of bis (2-methyl-1H-imidazol-3-ium) tetrachloridocobaltate (II). Acta Crystallographica, E71, 1064–1066. doi: 10.1107/S2056989015014127.

[31] Diop, M. B., Diop, L., Oliver, A. G. (2015). Crystal structure of bis(acetonyltriphenylphosphonium) tetrachloridocobaltate (II). Acta Crystallographica, E71, m209–m210. doi: 10.1107/S2056989015019180.

[32] Apex2, Crystallographic Software, Suite, Bruker AXS Inc., Madison, Wisconsin (USA) 2014.

[33] Krause, L., Herbst-Irmer, R., Sheldrick, G. M. and Stalke, D. (2015): Comparison of silver and molybdenum microfocus X-ray sources for single-crystal structure determination. Journal of Applied Crystallography, 48, 3–10.

[34] SAINT (Version 8.34A), Area Detector Integration Software, Bruker AXS Inc., Madison, Wisconsin, USA, 2014.

[35] Sheldrick, G. M. (2015). SHELXT-Integrated space-group and Crystal structure determination. Acta Crystallographica, A71 (1), 3–8. doi: 10.1107/S2053273314026370.

[36] Sheldrick, G. M. (2015). Crystal structure refinement with SHELXL. Acta Crystallographica, C71 (1), 3–8. doi: 10.1107/S2053229614024218.

[37] de Meulenaer, J., Tompa, H. (1965). The absorption correction in crystal structure analysis. Acta Crystallographica, 19 (6), 1014–1018. doi: 10.1107/S0365110X65004802.

[38] Sheldrick, G. M. (2008). A short history of SHELX. Acta Crystallographica, A64, 112–122. doi: 10.1107/S0108767307043930.

[39] Dolomanov, O. V., Bourhis, L. J., Gildea, R. J., Howard, J. A. K., Puschmann, H. (2009). OLEX2: a complete structure solution, refinement and analysis program, Journal of Applied Crystallography, 42 (2), 339–341. doi: 10.1107/S0021889808042726.

[40] Macrae, C. F., Bruno, I. J., Chisholm, J. A., Edgington, P. R., McCabe, P., Pidcock, E., Rodriguez-Monge, L., Taylor, R., van de Streek, J., Wood, P. A. (2008). Mercury CSD 2.0 – new features for the visualization and investigation of crystal structures. Journal of Applied Crystallography, 41 (2), 466-470. doi: 10.1107/S0021889807067908.

[41] Worley, C., Yangui, A., Roccanova, R., Du, M.-H., Saparov, B. (2019). $(CH_3NH_3)AuX_4 \cdot H_2O$ (X=Cl, Br) and $(CH_3NH_3)AuCl_4$: Low-Band Gap Lead-Free Layered Gold Halide Perovskite Materials, Chemistry–A European Journal, 25 (42), 9875-9884. doi: 10.1002/chem.201901112.